

NASA/TM—2007-214681



# Crew Exploration Vehicle (CEV) Water Landing Simulation

*Justin D. Littell*  
*University of Akron, Akron, Ohio*

*Charles Lawrence and Kelly S. Carney*  
*Glenn Research Center, Cleveland, Ohio*

## NASA STI Program . . . in Profile

Since its founding, NASA has been dedicated to the advancement of aeronautics and space science. The NASA Scientific and Technical Information (STI) program plays a key part in helping NASA maintain this important role.

The NASA STI Program operates under the auspices of the Agency Chief Information Officer. It collects, organizes, provides for archiving, and disseminates NASA's STI. The NASA STI program provides access to the NASA Aeronautics and Space Database and its public interface, the NASA Technical Reports Server, thus providing one of the largest collections of aeronautical and space science STI in the world. Results are published in both non-NASA channels and by NASA in the NASA STI Report Series, which includes the following report types:

- **TECHNICAL PUBLICATION.** Reports of completed research or a major significant phase of research that present the results of NASA programs and include extensive data or theoretical analysis. Includes compilations of significant scientific and technical data and information deemed to be of continuing reference value. NASA counterpart of peer-reviewed formal professional papers but has less stringent limitations on manuscript length and extent of graphic presentations.
- **TECHNICAL MEMORANDUM.** Scientific and technical findings that are preliminary or of specialized interest, e.g., quick release reports, working papers, and bibliographies that contain minimal annotation. Does not contain extensive analysis.
- **CONTRACTOR REPORT.** Scientific and technical findings by NASA-sponsored contractors and grantees.

- **CONFERENCE PUBLICATION.** Collected papers from scientific and technical conferences, symposia, seminars, or other meetings sponsored or cosponsored by NASA.
- **SPECIAL PUBLICATION.** Scientific, technical, or historical information from NASA programs, projects, and missions, often concerned with subjects having substantial public interest.
- **TECHNICAL TRANSLATION.** English-language translations of foreign scientific and technical material pertinent to NASA's mission.

Specialized services also include creating custom thesauri, building customized databases, organizing and publishing research results.

For more information about the NASA STI program, see the following:

- Access the NASA STI program home page at <http://www.sti.nasa.gov>
- E-mail your question via the Internet to [help@sti.nasa.gov](mailto:help@sti.nasa.gov)
- Fax your question to the NASA STI Help Desk at 301-621-0134
- Telephone the NASA STI Help Desk at 301-621-0390
- Write to:  
NASA Center for AeroSpace Information (CASI)  
7115 Standard Drive  
Hanover, MD 21076-1320

NASA/TM—2007-214681



# Crew Exploration Vehicle (CEV) Water Landing Simulation

*Justin D. Littell*  
*University of Akron, Akron, Ohio*

*Charles Lawrence and Kelly S. Carney*  
*Glenn Research Center, Cleveland, Ohio*

National Aeronautics and  
Space Administration

Glenn Research Center  
Cleveland, Ohio 44135

---

May 2007

Trade names and trademarks are used in this report for identification only. Their usage does not constitute an official endorsement, either expressed or implied, by the National Aeronautics and Space Administration.

*Level of Review:* This material has been technically reviewed by technical management.

Available from

NASA Center for Aerospace Information  
7115 Standard Drive  
Hanover, MD 21076-1320

National Technical Information Service  
5285 Port Royal Road  
Springfield, VA 22161

Available electronically at <http://gltrs.grc.nasa.gov>

# **Crew Exploration Vehicle (CEV) Water Landing Simulation**

Justin D. Littell  
University of Akron  
Akron, Ohio 44325

Charles Lawrence and Kelly S. Carney  
National Aeronautics and Space Administration  
Glenn Research Center  
Cleveland, Ohio 44135

## **Abstract**

Crew Exploration Vehicle (CEV) water splashdowns were simulated in order to find maximum acceleration loads on the astronauts and spacecraft under various landing conditions. The acceleration loads were used in a Dynamic Risk Index (DRI) program to find the potential risk for injury posed on the astronauts for a range of landing conditions. The DRI results showed that greater risks for injury occurred for two landing conditions; when the vertical velocity was large and the contact angle between the spacecraft and the water impact surface was zero, and when the spacecraft was in a toe down configuration and both the vertical and horizontal landing velocities were large. Rollover was also predicted to occur for cases where there is high horizontal velocity and low contact angles in a toe up configuration, and cases where there was a high horizontal velocity with high contact angles in a toe down configuration.

## **Introduction**

In order to assess the risks of a Crew Exploration Vehicle (CEV) water landing, a detailed study has been done using a combination of landing scenarios. These landing scenarios simulate the types of conditions that the CEV is expected to incur during normal and extreme landing conditions. These various normal and extreme conditions are simulated by adjusting CEV velocities, orientation, and angle of contact with the water. For each set of landing conditions a transient dynamic simulation is performed; resulting acceleration profiles are extracted and then used to determine astronaut injury risk levels using a human body injury model.

## **CEV Simulation Conditions**

A simple finite element model of the CEV and LS-DYNA, a commercial explicit finite element analysis code, was used for all simulations. For details on the development of this model, see appendix A. Ideally, a detailed CEV model with internal structure and elastic properties would be implemented to simulate these conditions; however, at the time of this study the design was not complete, so no detailed model was available. Therefore, simplifications to the model were made to speed up the run times while trying to retain as much detail as possible. As appendix A shows, the CEV model used in this study consists of a rigid outer CEV shell having no internal structure, with the appropriate inertial properties explicitly defined. The results from each simulation are output at the CEV center of gravity and post processed accordingly.

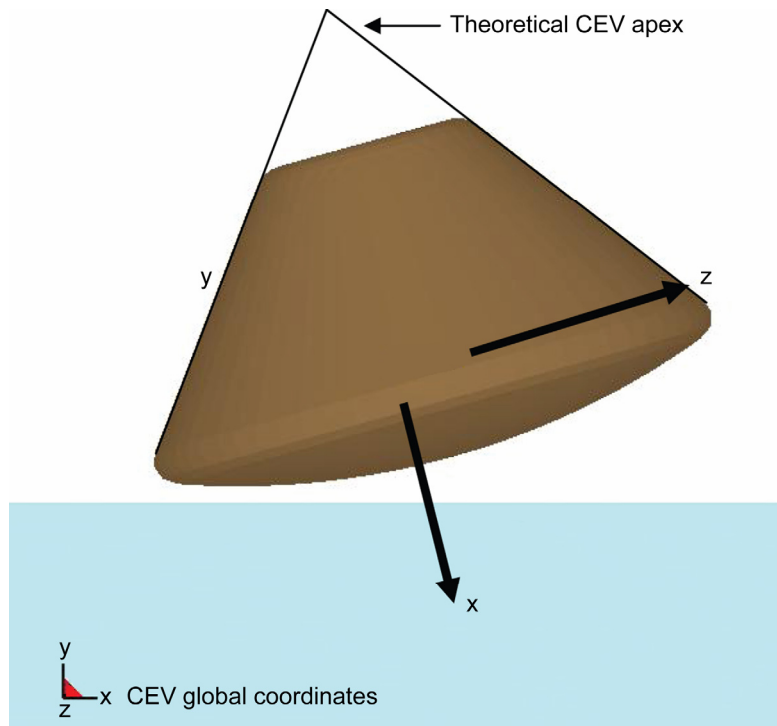


Figure 1.—CEV model with coordinate systems defined.

The CEV center of gravity (CG) location was defined from the theoretical CEV apex. The CG was located 134 in. below the theoretical CEV apex and 11.5 in. off center in the local Z direction. A local coordinate system was defined by positive X from CEV apex to CEV heat shield, positive Z from crewmembers feet to crewmembers head, and right-hand rule defined Y. The local coordinate system was added to the model by adding two extra nodes, which are attached to the CEV part and move along with the part. The purpose of defining a coordinate system in this manner was so the generated acceleration profiles can be readily used by the software that determines astronaut injury risks. A picture of the CEV model with local and global coordinate system and the water is shown in figure 1.

The astronaut pallet which carries the astronaut seats during landing was located below the CEV CG, in the local positive x direction. Since the CEV model did not have any internal structure and accelerations were only computed at the CEV CG, the accelerations were transformed to the location of the astronaut pallet for the injury risk calculations.

The finite element mesh is shown in figure 2. This model contained a total of 441 330 nodes. The model elements consisted of 8704 shell elements for the CEV skin, and 414 720 solid elements for the water and air mesh. The CEV skin was modeled as a rigid structural component with inertial properties (in LS-DYNA, MAT\_RIGID) representative of the CEV design. The rigid skin did not take into account the elastic properties of the spacecraft, which leads to bounding, conservative results. The water was modeled with appropriate properties, while the air was modeled as a void in which the water would be able to flow (in LS-DYNA the water was represented using MAT\_NULL and the air INITIAL\_VOID\_PART). Initial CEV velocities were imposed on the model in the X and Y global coordinates (in LS-DYNA, INITIAL\_VELOCITY\_RIGID\_BODY), and gravity was simulated (in LS-DYNA, LOAD\_BODY\_Y). For post-processing, accelerations at the CG were output in the local CEV coordinate system as defined in figure 1 (in LS-DYNA, DATABASE\_HISTORY\_NODE\_LOCAL).

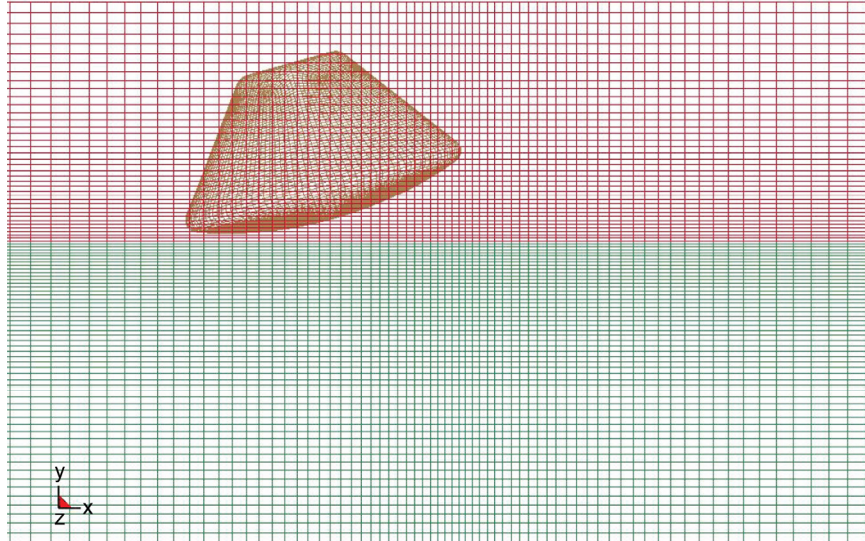


Figure 2.—CEV mesh.

## Configurations

Four parameters were varied in the splashdown analysis; vertical velocity, horizontal velocity, contact angle, and CEV orientation with respect to the CG. The *vertical velocity* is determined by how the parachutes were deployed and the number of working parachutes. The vertical velocity of 288 in./sec (24 fps) was the nominal case where all three parachutes deployed, 348 in./sec (29 fps) was for a two-parachute deployment, and 492 in./sec (41 fps) for a one-parachute deployment. Different vertical velocities were examined to assess the effect of a different number of parachute failures. (In the case of Apollo 15, only two out of the three possible parachutes actually deployed, as shown in fig. 3.)

The *horizontal velocity* was composed of two components: (1) the wind velocity and (2) the water velocity. These two components were combined and treated as a single horizontal velocity. The three horizontal velocity conditions studied were 0 in./sec (0 fps) corresponding to nominal conditions, 552 in./sec (46 fps) corresponding to Sea State 6 (5) and 720 in./sec (60 fps) in an extreme condition.

The *contact angle* was the relative angle between the CEV and the surface of the water. This was also a combination of two components: (1) hang angle (the angle in which the CEV is tilted due to parachute attachment location and drag) and (2) sea angle (the angle of the water surface due to waves). These two components are combined and identified as contact angle. Four contact angle conditions were examined: 0°, 15°, 27.5°, and an extreme case of 60°. These angles are measured about the CEV local Y axis.

The *CEV orientation with respect to the CG* was a designation used to determine whether the CEV would land toe down or toe up. These two conditions can be best illustrated by figure 4.

Figure 4 depicts the CEV landing orientations used for the present analysis. Two other directions could have also been examined (toe down with CG (–) and toe up with CG (+)), but due to time constraints, these were omitted. The two configurations shown in the figure were picked because the same conditions were tested with Apollo capsules (ref. 2). By performing landing simulations under similar conditions, comparisons between Apollo and CEV can be made. The left picture shows a condition of a toe up, CG negative configuration. Under this condition, the rear portion of the heat shield impacts the water first. The right picture shows a condition of a toe down, CG positive analysis. This represents the



Figure 3.—Apollo 15 splashdown with only two parachutes deployed.

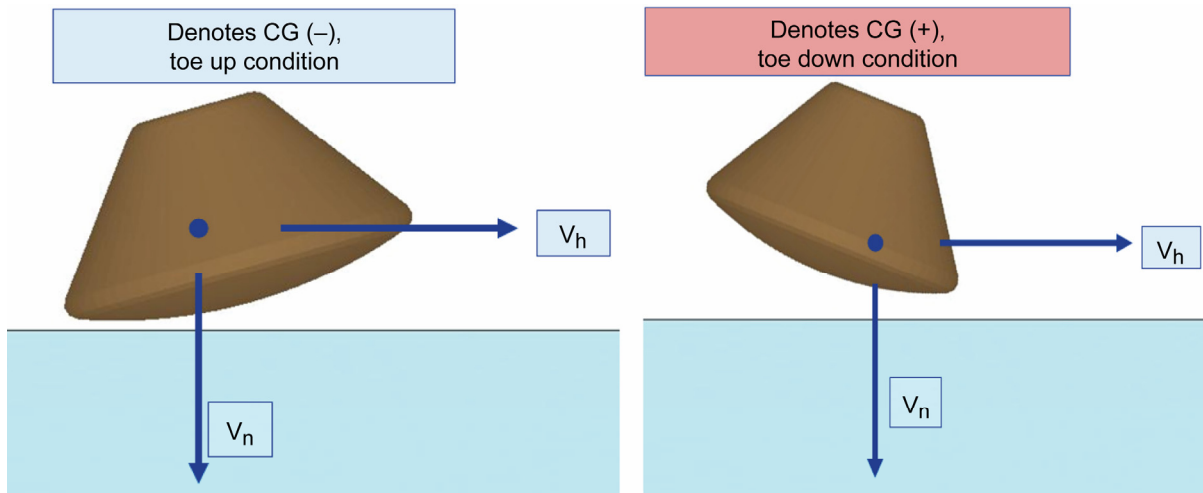


Figure 4.—CG locations for CEV splashdown.



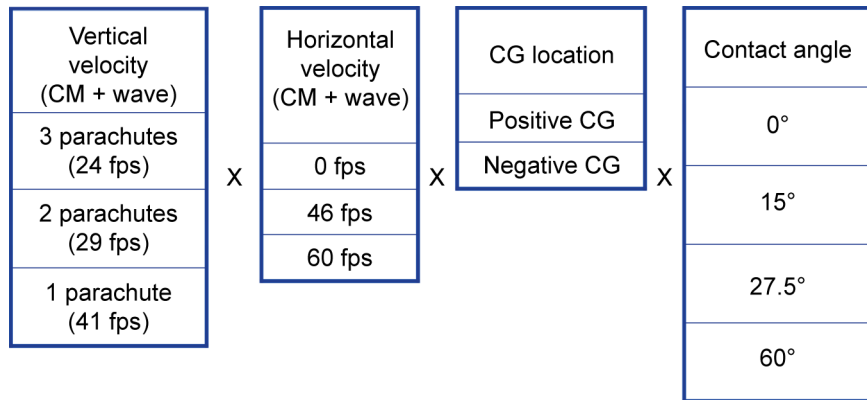


Figure 5.—CEV configuration matrix.

CEV cutting into the water with its leading edge. Notice that the toe in these cases represents the leading edge of the CEV. For brevity, when the CG is on the negative Z side of the local CEV coordinate system, the nomenclature will be CG negative and when the CG is on the positive Z side in the local CEV coordinate system, the nomenclature will be CG positive. This terminology will be used for the remainder of this report.

The landing configuration matrix is shown in figure 5. A total of 72 combinations were possible; however, a subset of cases were picked as a representation of the entire set and only these cases were simulated.

### Dynamic Response Index (DRI)

DRI is an accepted index used to predict injury to human occupants during impact events. In the present study, the DRI was used to predict astronaut injury for healthy astronauts during a spacecraft water landing. The health condition of the astronauts affects the predicted index since less than healthy humans are more susceptible to risk during impact events such as vehicle landings. The DRI software program incorporated a spring mass damper model for the astronaut and seat then used LS-DYNA pallet accelerations as input and computed the acceleration levels felt by the astronaut along with risk levels based off the Brinkley model. Since the DRI program uses time history acceleration data, cases with the maximum LS-DYNA acceleration loads do not necessarily produce the highest risk if the maximum acceleration is extremely short. Rather, moderate LS-DYNA acceleration levels that last for longer periods of time sometimes lead to higher risk levels.

The DRI was direction dependent and had different acceptable risk levels for each of the three primary directions. The three directions were referred to as “eyeballs in” (+X), “eyeballs out” (-X), “eyeballs left” (-Y), “eyeballs right” (+Y), “eyeballs up” (+Z), and “eyeballs down” (-Z). The head of the astronaut was positioned in the headrest shown to the right of figure 6 and the feet protruded out to the left of the seat.

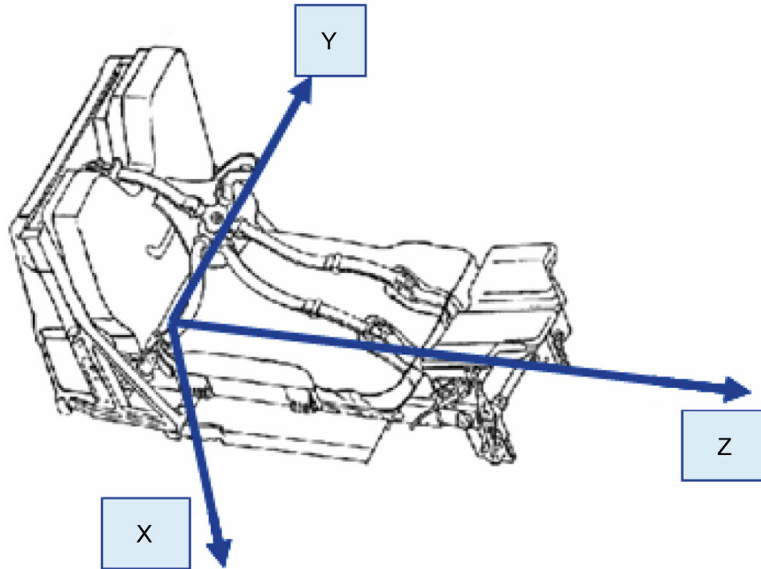


Figure 6.—DRI risk directions.

## Rollover

The potential for CEV rollover during water landings was also examined in this study. Due to the limited timeframe for this study and the computational time required for completing full runs, rollover was predicted for most cases without performing complete analytical simulations. In most cases, rollover predictions were made by examining the LS-DYNA animations in conjunction with the time history plots of the rotation angles and rotational velocities and accelerations of the CEV vehicle. In cases where rollover was probable, models were rerun for a longer time duration, which would capture the capsule rollover.

## Computational Resources

The LS-DYNA simulations were run on an eight-node LINUX cluster running LS-DYNA 970 in single precision. The specified termination time for each simulation was 0.5 sec. A single simulation took approximately 24 hours to complete using this eight-node LINUX cluster. Since LS-DYNA allowed for the viewing of results while the job was running, many of the models where it was determined that the acceleration levels had already peaked were prematurely terminated before the full 0.5 sec was reached. D3PLOT files (LS-DYNA output) were written every 0.01 sec and all acceleration data was written every  $10^{-4}$  sec. A total of 54 landing cases were run.

Models used to predict rollover were run on the Columbia computing cluster at the NASA Ames Research Center (ref. 7) with a 32-node LINUX cluster in single precision. The termination time for these models was 3 sec. This was enough time to capture capsule rollover.

## Results

All results were post processed using LS-PREPOST v2. Nodal accelerations were extracted at node 900 000 (CEV CG) for the x, y, z, and ry (y-rotation) directions. The CG accelerations were transformed to the astronaut location because data was needed at the astronaut pallet location. The accelerations were filtered at 100 Hz and divided by  $386.4 \text{ in./sec}^2$  to obtain results in units of gravity instead of  $\text{in./sec}^2$ .

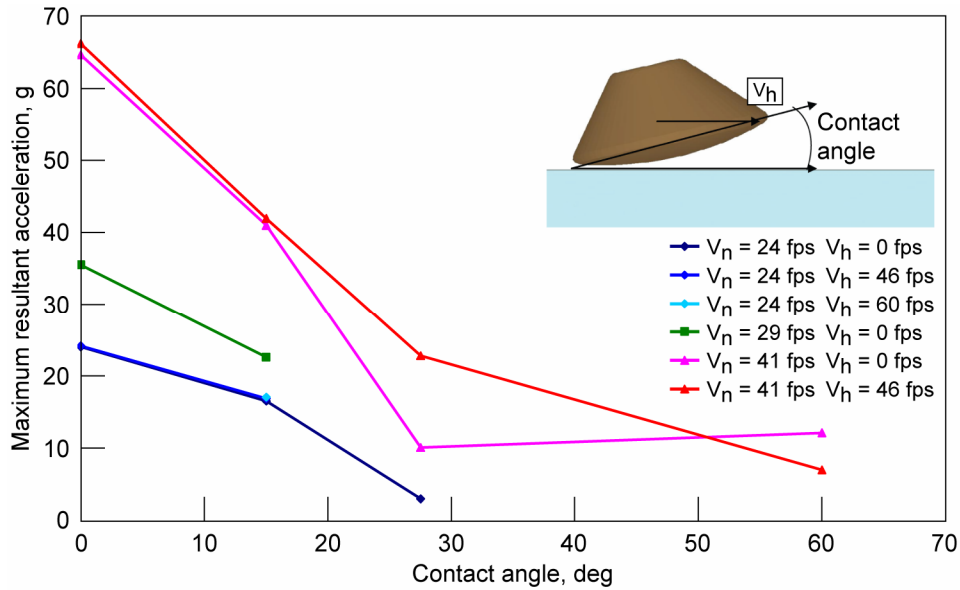


Figure 7.—Maximum resultant acceleration versus contact angle for CG negative positions.

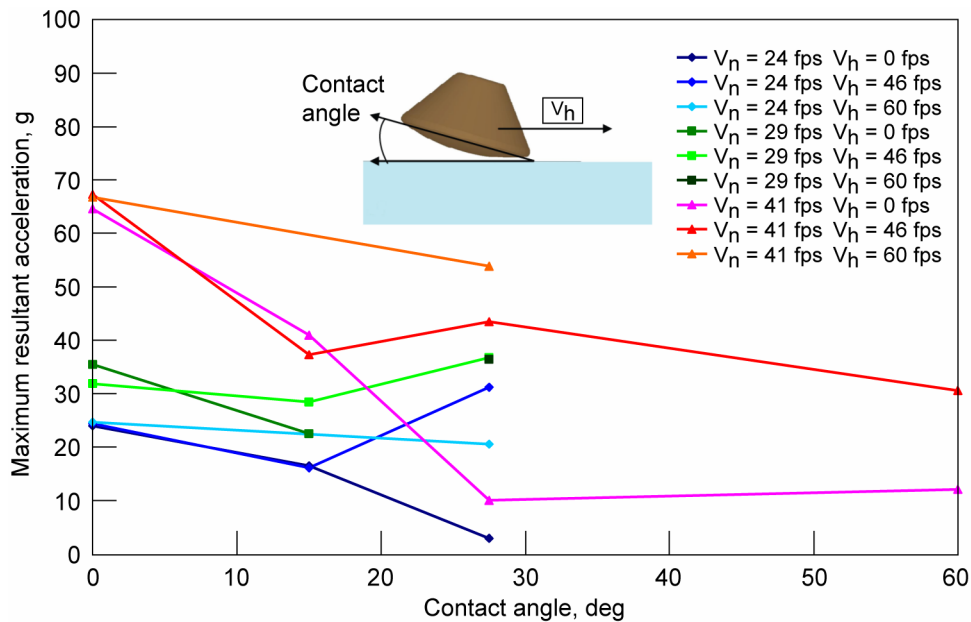


Figure 8.—Maximum resultant acceleration versus contact angle for CG positive positions.

Figure 7 shows resultant acceleration versus contact angle with a negative CG orientation (toe up) and at different vertical velocities. Three pieces of information can be obtained from figure 7. First, when the contact angle was low, the resultant accelerations were at a maximum. As the contact angle was increased to 60°, the maximum resultant accelerations leveled off toward a minimum. The data points between low and high contact angle followed a parabolic trend similar to figure 3 in reference 3. Also, as vertical velocity increased, the maximum resultant acceleration also increased. The worst case was a vertical velocity of 41 fps with a contact angle of 0°. In general, for the toe up configuration, horizontal velocity did not have a significant effect on the resulting accelerations.

Figure 8 shows resultant acceleration versus contact angle for a negative CG orientation (toe down) and at different vertical velocities. When the contact angle was at a minimum (i.e., zero), the resultant

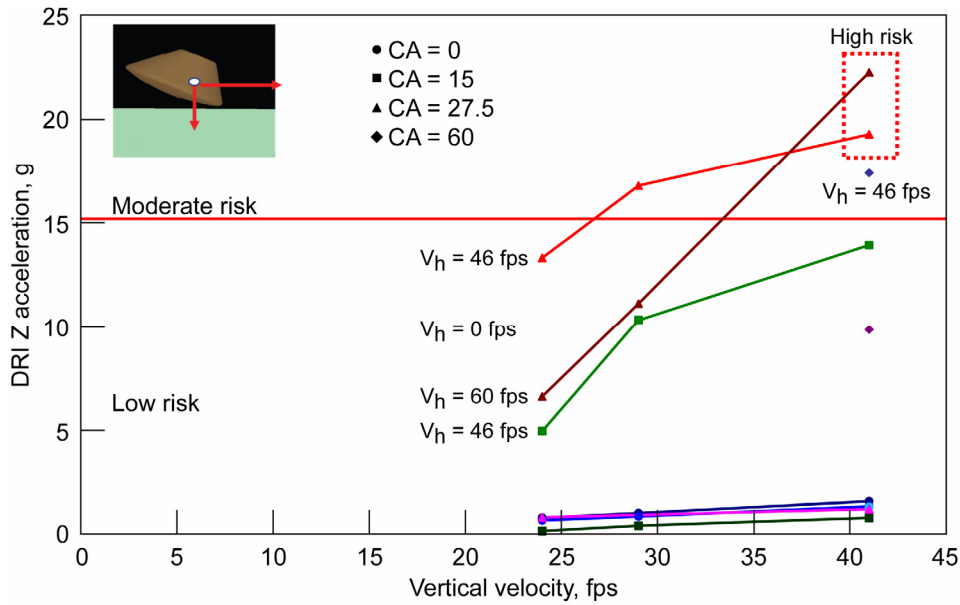


Figure 9.—Z DRI levels for CG positive position.

acceleration was at a maximum. The difference from the toe up configuration; however, was that for this configuration, horizontal velocity had an effect on the maximum resultant acceleration. For example, at a contact angle of  $27.5^\circ$  with a vertical velocity of 41 fps, the data ranged from between approximately 10 and 54 g. No definite conclusions could be made for contact angles beyond  $27.5^\circ$  since only limited data were obtained beyond this range.

Figure 9 shows the DRI in the eyeballs up/down (spinal) direction as a function of vertical velocity for a positive CG orientation (toe down). The “moderate” box shown in the figure delineates the cutoff line for moderate risk conditions; anything above this line represents moderate risk. The “high” box mark points to high risk. The spinal direction proved to be the worst case for astronaut risk while the other directions only exhibited low levels of risk. For the spinal direction there were three data points that exhibited greater than low levels of risk. At contact angles higher than  $27.5^\circ$  and at vertical velocities of 29 fps and above, the DRI showed moderate- and high-risk levels.

Figure 10 shows the motion of the CEV under the following conditions: 41 fps vertical velocity, 46 fps horizontal velocity, positive CG orientation (toe down) and  $27.5^\circ$  contact angle. This configuration corresponds to the lower “high risk” red triangle in figure 10. As the CEV cut through the water, the local CEV Z direction incurred the largest deceleration. This large deceleration was the primary contributor to the high-risk DRI. The other moderate and high DRI cases have similar landing characteristics to figure 10.

Figure 11 shows X-axis (eyeballs in/out) DRI acceleration levels for a positive CG orientation (toe down). For this configuration, the lower contact angles produced the largest accelerations and risk levels. At a contact angle of  $0^\circ$ , a moderate DRI risk was generated whereas all other levels of risk were low. There are three blue circles near or above the moderate risk index line in the upper right corner of figure 12. These corresponded to cases of 41 fps vertical velocity,  $0^\circ$  contact angle, positive CG location, but different horizontal velocities. All of the data was clustered similarly. Comparing this to figure 9, data that has low Z DRI acceleration ( $0^\circ$  contact angle cases) had high X DRI acceleration and data that has high Z DRI acceleration (big contact angle cases) had low X DRI acceleration.

Figure 12 shows X DRI acceleration for all cases with a negative CG configuration (toe up). All cases ran showed a low risk. The  $0^\circ$  contact angle data approached moderate risk; however, moderate risk was not reached. Figure 13 illustrates the CEV impact for the worst condition in figure 12, which is a vertical velocity of 41 fps, horizontal velocity of 46 fps, a negative CG orientation and a contact angle of  $0^\circ$ . This

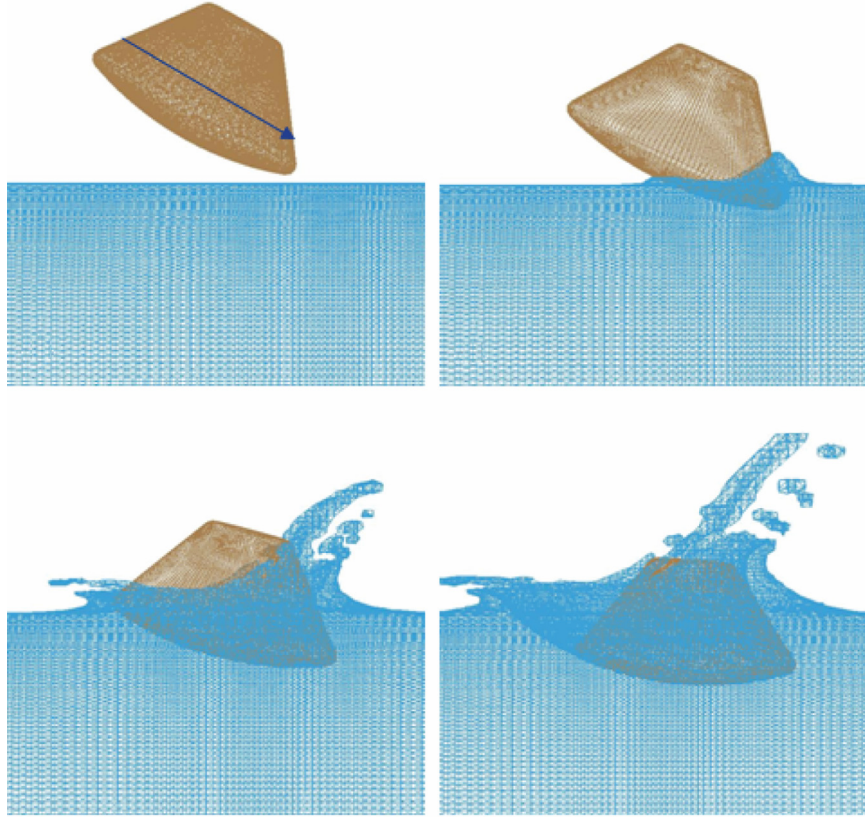


Figure 10.—CEV landing ( $V_n = 41$  fps  $V_n$ ,  $V_h = 46$  fps, positive CG, CA = 27.5°).

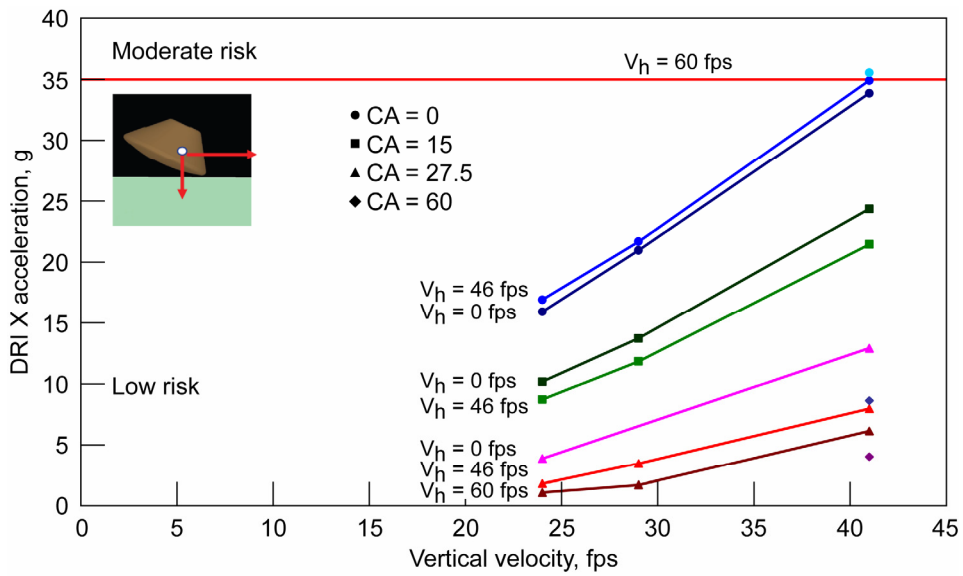


Figure 11.—X DRI levels for CG positive position.



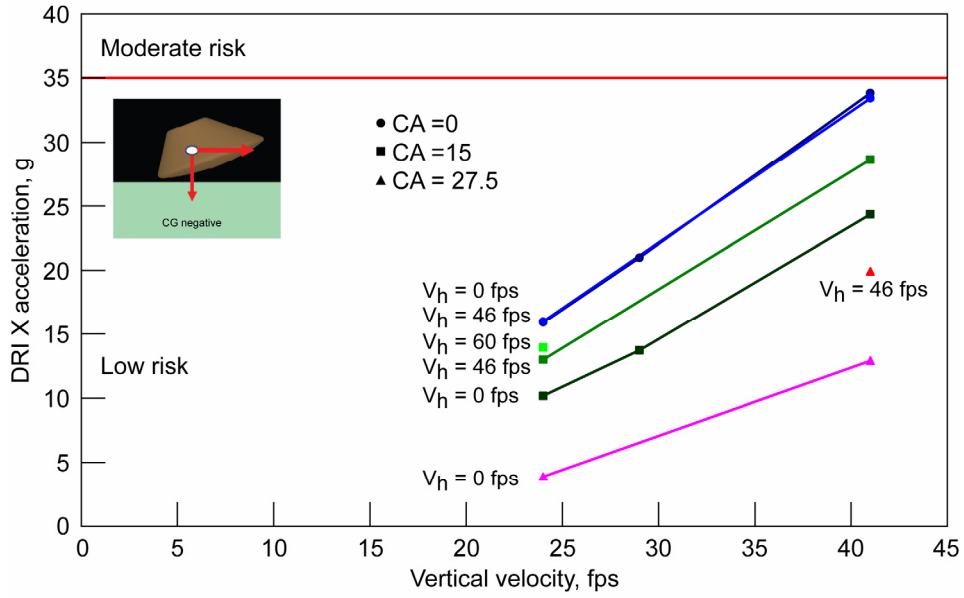


Figure 12.—X DRI levels for CG negative position.

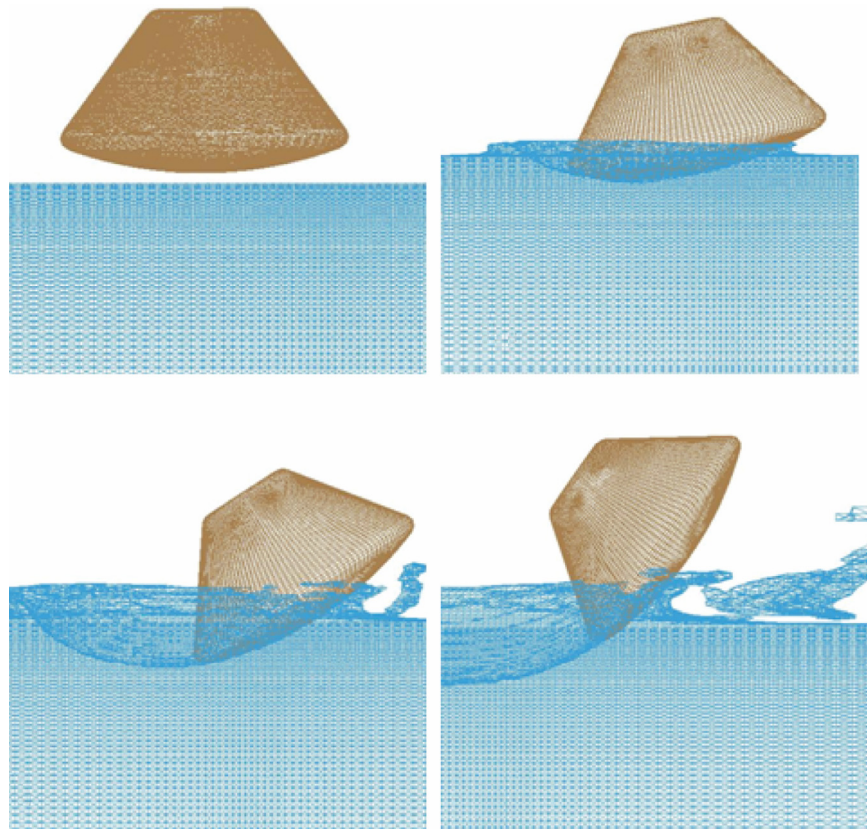


Figure 13.—CEV landing ( $V_n = 41$  fps,  $V_h = 46$  fps, negative CG, CA = 0°).

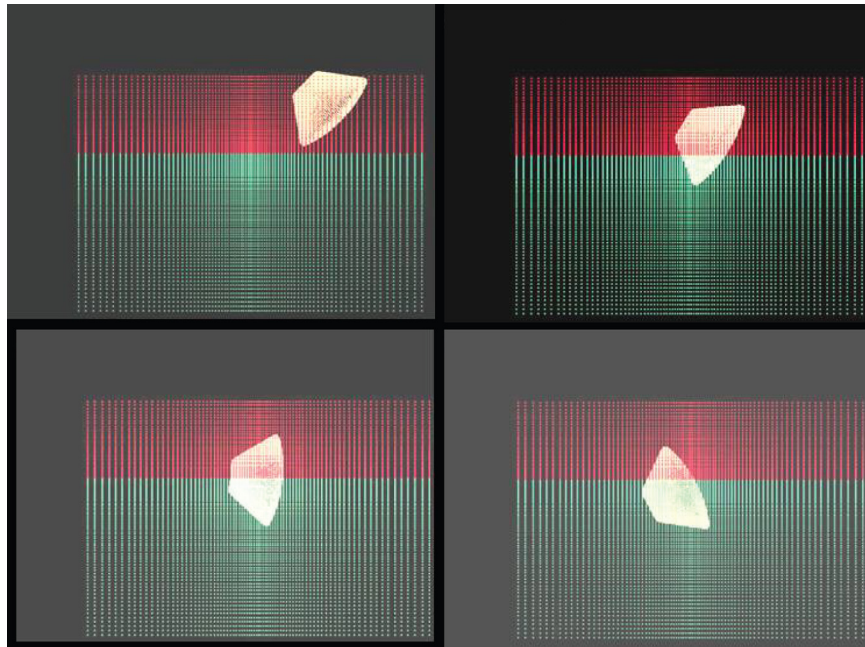


Figure 14.—CEV rollover ( $V_n = 24$  fps,  $V_h = 46$  fps, positive CG, CA =  $45^\circ$ ).

configuration was also investigated to see if rollover occurred, and was found that it did not. Figure 12 is similar to figure 11; however, acceleration levels are slightly less.

## Rollover

In cases where it looked like rollover was a possibility, longer duration simulations were run on the Ames Research Center Columbia computing cluster. The Ames cluster was used because of its superior computing power and ability to run longer simulations with shorter turnaround times. Rollover cases were examined for a CG positive configuration (toe up). Simulations completed at Ames indicated that the CEV rolled over when the contact angle was greater than  $45^\circ$  and the horizontal velocity was high. The two cases run with a vertical velocity of 24 fps, horizontal velocity of 46 fps, and contact angles of  $45^\circ$  and  $60^\circ$  both rolled over. In figure 14, the CEV reached maximum accelerations at 0.5 sec, and has rolled over (bottom right picture).

## Conclusions

A CEV water model was generated and run with LS-DYNA. Because the actual landing conditions of the CEV cannot be definitely predicted or planned, the worst conditions were examined and reported.

The results show that with all three parachutes functioning, there was a low risk for injury for the astronauts for all conditions. With 2 parachutes functioning, 1 case out of 10 gave moderate risk conditions. With only 1 parachute functioning, 2 cases out of 23 gave moderate risk and 2 cases out of 23 gave high risk.

All five cases that gave moderate or high risk occurred when the CEV was in the positive CG position (toe up). Four out of the five cases occurred when the CEV had a high contact angle, high horizontal velocity, and high vertical velocity. These were basically off-nominal or worst-case-type scenarios. In these four cases, the Z DRI acceleration (spinal) dominated the risk criteria. The final case occurred when the CEV had a low contact angle and high vertical velocity. This was the only case where the X DRI acceleration (eyeballs in/out) dominated the risk criteria.

Further investigations showed that since DRI accelerations are direction dependent, when the contact angle was high, the maximum resultant acceleration went down, but the Z DRI index went up, leading to higher risk. At low contact angles, the Z acceleration was low but the X acceleration was high. However, since the limit for the X DRI direction was much higher than the limit for the Z DRI acceleration, the risks were still low.

In most cases, maximum astronaut DRI accelerations were between 50 and 80 percent of actual CEV pallet accelerations, but in certain cases, due to the DRI's dependence on the acceleration time history, the DRI was greater than pallet accelerations.

Rollover conditions were examined, and the cases that had low contact angle with high vertical and horizontal velocity in a negative CG configuration also showed the potential for rollover. Cases where the contact angle was low in a negative CG configuration did not show the capsule rolling over.



## Appendix A—CEV Model Developments

An Apollo spacecraft water landing model was developed by Al Tabiei (University of Cincinnati) for the purpose of providing a high-fidelity simulation capability to predict spacecraft water landings using LS-DYNA. This model was subsequently provided to NASA Glenn Research Center (Glenn) for performing water landing simulations for the planned Crew Exploration Vehicle (CEV). The original model contained an Apollo spacecraft and a water and an air mesh. The Apollo spacecraft part was modeled as a rigid shell having no internal structure and would be the starting point for developing the CEV model. When developing the CEV from this Apollo model, inertial properties were added to the model by creating a node at the theoretical CEV center of gravity (CG), assigning this node appropriate CEV inertia properties and constraining this node to the spacecraft part.

An Arbitrary-Lagrangian-Eulerian (ALE) approach was used with LS-DYNA for performing the water landing simulations. This allowed for a Lagrangian mesh (rigid spacecraft) to move freely within a stationary Eulerian mesh (water and air). Contact forces between the spacecraft and water impact surface and spacecraft accelerations were output and examined. The ALE mesh was approximately five times the length, three times the height, and two times the width of the actual Apollo capsule. This mesh was deemed large and dense enough to accurately capture the spacecraft impact behavior while minimizing the required computational efforts.

The supplied Apollo model was in metric units, but for this analysis the model needed to be converted to English units. This conversion was done by scaling all lengths by 39.37 (the conversion from meters to inches) and converting all of the material properties into the appropriate English equivalent. The most critical item needed for conversion was the Gruneisen Equation of State (EOS) model. In general, EOS is the governing equations for the behavior of the water undergoing shock, but for this situation, correct EOS values were needed to accurately simulate the impact between the capsule and water. English equivalents for the Gruneisen EOS were obtained from Meyers. These values are as follows:  $C = 64840$ ,  $S1 = 2.56$ ,  $S2 = -1.986$ ,  $S3 = 0.2268$ , and  $\Gamma = 0.5$ .

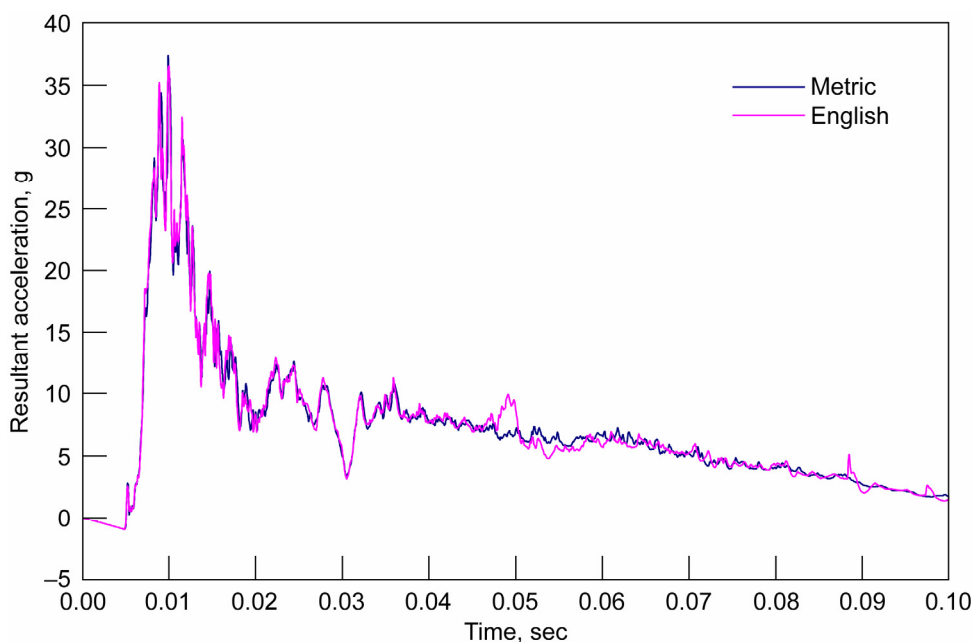


Figure A1.—Metric versus English Apollo conversion.

TABLE A1.—FPS TO IPS MOMENT OF INERTIA CONVERSIONS

FPS, slug-ft <sup>2</sup>	Conversion <sup>a</sup>	IPS, lb-in. <sup>2</sup>
I <sub>xx</sub> = 8500	32.17 lb/slug * 144 in. <sup>2</sup> /ft <sup>2</sup> *1/386.4 <sup>2</sup>	101904
I <sub>yy</sub> = 6650		79725.6
I <sub>zz</sub> = 6150		73731.2
I <sub>xy</sub> = 275		3296.9
I <sub>xz</sub> = -350		-4196
I <sub>yz</sub> = 0		0

<sup>a</sup>Note that the conversion of mass units from slug to pound mass needs a division by 386.4 (gravity in in./sec<sup>2</sup>). When a gravity load is applied to the model, the division cancels out leaving mass and weight in the correct units.

The Apollo CG resultant accelerations, after conversion into English units, were compared to the original metric resultant accelerations.

After the original Apollo model was converted into English units, the capsule model was modified to reflect the CEV properties. Most importantly, the size and the inertia properties were updated. The Apollo was scaled from 12 ft (144 in.) to 16.5 ft (198 in.). The inertia properties were taken from the DAC-II configuration. The provided CEV DAC-II units were converted from the foot-slug-second (FSS) unit system to an in.-lb-sec (IPS) unit system.

## References

1. Meyers, M.: Dynamic Behavior of Materials. John Wiley & Sons, 1994.
2. Stubbs, S.: Dynamic Model Investigation of Water Pressures and Accelerations Encountered During Landings of the Apollo Spacecraft. NASA TN D-3980, 1967.
3. NASA. Landing Impact Attenuation for Non-Surface-Planing Landers. NASA SP-8046, 1970.
4. Tutt, B.; and Taylor, A.: The Use of LS-DYNA to Simulate the Water Landing Characteristics of Space Vehicles. 8th International LS-DYNA Users Conference.
5. Bourassa, M.A.; Vincent, D.G.; Wood, W.L.: A Flux Parameterization Including the Effects of Capillary Waves and Sea State. *J. Atmos. Sci.*, vol. 56, 1999, pp. 1123-1139.
6. Carney, Kelly and Lawrence, Charles (NASA Glenn), and Ed Fascenella (NASA Langley). Personal Conversations.
7. Levitt, Creon: NASA Ames Research Center. Personal conversations.

**REPORT DOCUMENTATION PAGE**

*Form Approved*  
OMB No. 0704-0188

The public reporting burden for this collection of information is estimated to average 1 hour per response, including the time for reviewing instructions, searching existing data sources, gathering and maintaining the data needed, and completing and reviewing the collection of information. Send comments regarding this burden estimate or any other aspect of this collection of information, including suggestions for reducing this burden, to Department of Defense, Washington Headquarters Services, Directorate for Information Operations and Reports (0704-0188), 1215 Jefferson Davis Highway, Suite 1204, Arlington, VA 22202-4302. Respondents should be aware that notwithstanding any other provision of law, no person shall be subject to any penalty for failing to comply with a collection of information if it does not display a currently valid OMB control number.

PLEASE DO NOT RETURN YOUR FORM TO THE ABOVE ADDRESS.

<b>1. REPORT DATE (DD-MM-YYYY)</b> 14-05-2007		<b>2. REPORT TYPE</b> Technical Memorandum		<b>3. DATES COVERED (From - To)</b>	
<b>4. TITLE AND SUBTITLE</b> Crew Exploration Vehicle (CEV) Water Landing Simulation				<b>5a. CONTRACT NUMBER</b>	
				<b>5b. GRANT NUMBER</b>	
				<b>5c. PROGRAM ELEMENT NUMBER</b>	
<b>6. AUTHOR(S)</b> Littell, Justin, D.; Lawrence, Charles; Carney, Kelly, S.				<b>5d. PROJECT NUMBER</b>	
				<b>5e. TASK NUMBER</b>	
				<b>5f. WORK UNIT NUMBER</b> WBS 843515.02.01.03.05.08.04	
<b>7. PERFORMING ORGANIZATION NAME(S) AND ADDRESS(ES)</b> National Aeronautics and Space Administration John H. Glenn Research Center at Lewis Field Cleveland, Ohio 44135-3191				<b>8. PERFORMING ORGANIZATION REPORT NUMBER</b> E-15831	
<b>9. SPONSORING/MONITORING AGENCY NAME(S) AND ADDRESS(ES)</b> National Aeronautics and Space Administration Washington, DC 20546-0001				<b>10. SPONSORING/MONITORS ACRONYM(S)</b> NASA	
				<b>11. SPONSORING/MONITORING REPORT NUMBER</b> NASA/TM-2007-214681	
<b>12. DISTRIBUTION/AVAILABILITY STATEMENT</b> Unclassified-Unlimited Subject Category: 18 Available electronically at <a href="http://gltrs.grc.nasa.gov">http://gltrs.grc.nasa.gov</a> This publication is available from the NASA Center for AeroSpace Information, 301-621-0390					
<b>13. SUPPLEMENTARY NOTES</b>					
<b>14. ABSTRACT</b> Crew Exploration Vehicle (CEV) water splashdowns were simulated in order to find maximum acceleration loads on the astronauts and spacecraft under various landing conditions. The acceleration loads were used in a Dynamic Risk Index (DRI) program to find the potential risk for injury posed on the astronauts for a range of landing conditions. The DRI results showed that greater risks for injury occurred for two landing conditions; when the vertical velocity was large and the contact angle between the spacecraft and the water impact surface was zero, and when the spacecraft was in a toe down configuration and both the vertical and horizontal landing velocities were large. Rollover was also predicted to occur for cases where there is high horizontal velocity and low contact angles in a toe up configuration, and cases where there was a high horizontal velocity with high contact angles in a toe down configuration.					
<b>15. SUBJECT TERMS</b> Spacecraft design; Landing; Astronauts; Risk					
<b>16. SECURITY CLASSIFICATION OF:</b>			<b>17. LIMITATION OF ABSTRACT</b>	<b>18. NUMBER OF PAGES</b> 21	<b>19a. NAME OF RESPONSIBLE PERSON</b> Charles Lawrence
<b>a. REPORT</b> U	<b>b. ABSTRACT</b> U	<b>c. THIS PAGE</b> U			<b>19b. TELEPHONE NUMBER (include area code)</b> 216-433-6048



